# STRUCTURAL INVESTIGATIONS OF CANDIDATE MATERIALS FOR TURBINE DISC APPLICATIONS BEYOND 700 °C

H.J. Penkalla, J. Wosik, W. Fischer, F. Schubert
Research Center Jülich, Institute for Materials and Processes in Energy Systems
D-52425 Jülich, Germany

#### Abstract

Three Ni-base wrought alloys with different hardening mechanisms (Inconel 706, Waspaloy and Inconel 617) are candidates for steam turbine disc applications with temperatures up to 700 °C and were examined in respect to their microstructure and microstructural stability. The materials were investigated after different heat treatments and after short and long term ageing by metallography, scanning and transmission electron microscopy. Special DTA experiments has been performed to confirm the known TTT diagrams and to study the initial precipitation of different phases and their growth, as function of cooling rate after the heat treatment. The amount and size of precipitations were evaluated by image analysis and stereological methods.

The Nb containing alloy Inconel 706 shows a complex microstructure containing  $\gamma$ ',  $\gamma$ '' and  $\eta$  phases which are stable under long term service up to 620 °C. At higher temperatures a strong particle coarsening and phase transformation was observed. Waspaloy is hardened by  $\gamma$ ' particles with a bimodal size distribution. After ageing at 700 °C and higher a coarsening was observed by loss of the bimodal size distribution. Inconel 617 is a solid solution hardened material additionally hardened by homogeneously distributed fine  $M_{23}C_6$  carbides. After long term ageing at temperatures of 650 °C to 750 °C the carbides tended to form carbide films along the grain boundaries and at 700 °C to 750 °C  $\gamma$ ' precipitated to homogeneously distributed particles with low coarsening under long term service.

#### Introduction

An increase in the efficiency of steam power plants can be reached by increasing the steam temperature. In future, power plant for electricity generation will, for thermal efficiency and ecological reasons, operate with steam temperatures as high as 700°C. The currently used martensitic/feritic steels are limited to application temperatures of about 620 °C [1]. Many existing polycrystalline nickel-base superalloys, used in the aerospace aircraft turbine engines could be principal used for this high temperatures, but they are not fabricable to heavy components and too expensive to be used in power plant components. Ni-base wrought superalloys with good formability, sufficient creep strength and creep crack growth resistance and high structure stability during long term service at the application temperatures may be candidate material for large components.

Within the context of a German DFG research project "Production and life time models for the application of Ni-base alloys in steam turbines at temperatures above 700 °C" different aspects of the use of Ni-base superalloys should be modeled. In order to collect a data base for the modeling, in a first screening step three candidates, Inconel 706, Inconel 617 and Waspaloy, have been investigated in respect to their casting, forgeability, heat treatment, structure and structural stability and mechanical properties such as creep strength and creep crack growth behavior in the temperature range of 650 to 750 °C.

An important criterion for these material selections was the differences in the hardening mechanisms of these alloys. Inconel 617 is representative for solid solution hardened Ni-base alloys, Waspaloy is hardened by coherent  $\gamma$  particles and Inconel 706 shows a complex microstructure with  $\gamma$ ,  $\gamma$ " and  $\eta$  phase. In the following contribution the aspects of the alloy structure and the structural stability will be reported.

#### **Experiments**

#### Materials and heat treatment

Inconel 706 is a Nb containing Ni-Fe-base superalloy derived from Inconel 718 with higher Fe and Ti content to improve the forgeability and to reduce the tendency for segregation [2-5]. The microstructure consists of fine  $\gamma$ ' and  $\gamma$ '' precipitates, homogeneously distributed in the  $\gamma$  matrix, and, depending on the heat treatment,  $\eta$ -phases along the grain boundaries as a cellular structure. Additionally M(C,N) carbonitrides can be found. Inconel 617 is a solid solution hardened material and shows after heat treatment a distribution of small M<sub>23</sub>C<sub>6</sub> precipitates in the matrix and along the grain boundaries. Waspaloy is hardened by  $\gamma$ ' precipitates in a bimodal size distribution of primary and secondary particles and a small part of M<sub>23</sub>C<sub>6</sub> particles, which tend to precipitate at the grain boundaries in a globular shape.

The chemical composition of the investigated alloys is shown in Table 1. From Inconel 706 three variants were investigated to observe the influence of the heat treatment and the Nb and C content on the amount and structure of precipitates. The variant Inconel 706 A and Inconel 706 B with the same nominal chemical composition obtained different heat treatments. Inconel 706 C has higher Nb and C concentrations and was heat treated like Inconel 706 B.

Table 1: Nominal chemical composition of Inconel 706, Inconel 617 and WASPALOY

Chemical composition wt%					
Element	Inconel 706A+B	Inconel 706 C	Inconel 617	Waspaloy	
Ni	42	42.46	54	57.1	
Fe	37.1	36.19	0.5	0.57	
Cr	16	16.04	22	19.35	
Ti	1.54	1.61	0.55	3.13	
Al	0.26	0.17	1.11	1.22	
Nb	2.96	3.33	0	0.01	
С	0.01	0.05	0.55	0.033	
В	0.0034		0.001	0.005	
Co			12.9	14	
Mo			9.05	4.52	
Si	0.05		0.14	0.04	

Inconel 706 A has been solution treated at 980 °C for 2 h with a following cooling down to room temperature at a cooling rate of 25 K/min (Figure 1). The subsequent precipitation annealing was performed at 720 °C for 8 h and at 620 °C for 8 h. This heat treatment results in a homogeneous distribution of small  $\gamma$ ' and  $\gamma$ '' precipitates, the  $\eta$  phase is absent.

In order to precipitate the  $\eta$  phase the heat treatment of variant Inconel 706 B was used. This heat treatment according to the results of Shibata [5] introduces a stabilizing step at 820 °C for 8 h following solution annealing. Different to the Shibata's heat treatment the stabilizing follows directly solution annealing by cooling down from 980 °C to 820 °C at a cooling rate of 4 K/min. This procedure should avoid initial  $\gamma$ ' and  $\gamma$ ' precipitation during the cooling down before  $\eta$  phase precipitates.

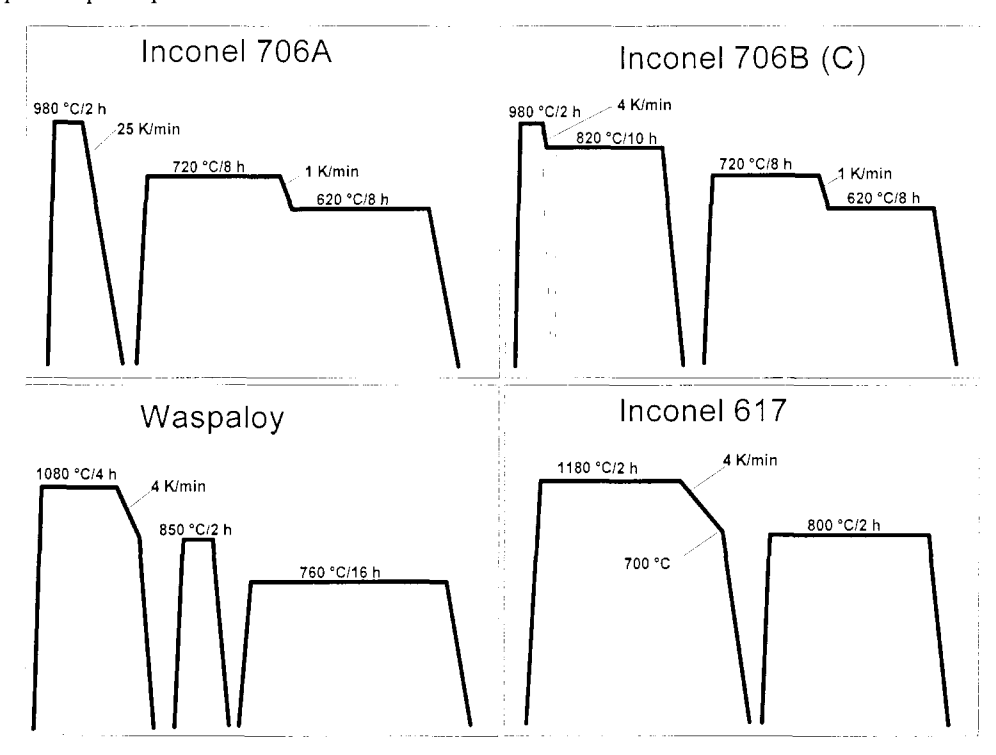


Figure 1: Heat treatments of the investigated alloys. The dashed lines indicate the heat treatment proposed by Shibata [5].

The heat treatment of Inconel 617 consist of two steps, an initial solution annealing at 1180 °C for 2 h and a precipitation annealing at 800 °C for 2 h. After the solution annealing the specimen was cooled down to room temperature. Down to 700 °C the cooling rate was limited to 4 K/min to avoid a supersaturation of C in the matrix. This procedure leads to a homogeneous distribution of  $M_{23}C_6$  during the stabilizing annealing. The temperature of 800 °C was chosen to avoid an additional  $\gamma$ ' precipitation, which may occur at heat exposure in the temperature range of 650 °C to 750 °C.

Waspaloy alloy was solution treated at 1080 °C for 4 h, followed by ageing at 850 °C for 2 h and at 760 °C for 16 h. Between the three annealing steps the specimen were cooled down to room temperature, particularly after the solution annealing up to 700 °C with a cooling rate of 4 K/min.

Table 2 shows the grain size and hardness HV10 of the investigated materials. The  $\gamma$ ' and  $\gamma$ '' hardened Inconel 706 A shows the highest value of hardness. The  $\eta$  phase in the variants Inconel 706 B and Inconel 706 C leads to a loss of hardness of about 10%.

Material	mean grain size (μm)	hardness HV10	
Inconel 706 A	39	426	
Inconel 706 B	69	378	
Inconel 706 C	130	376	
Inconel 617	223	169	
Waspalov	44	328	

<u>Table 2:</u> Grain size and hardness of the investigated alloys

# Methods of investigations

The microstructural investigations were carried out using scanning and transmission electron microscopy (SEM, TEM). The preparation of thin foil specimens for TEM examinations were mechanically thinned to about 80  $\mu$ m thickness, followed by double jet polishing (Tenupol) to 5  $\mu$ m residual thickness in the etching dimple. The last step of thinning was done by small-angle ion beam milling (Gatan PIPS) with angles of -3, and +4° and an energy of 5keV. The conditions of the electrolytic polishing process were: temperature -25°C, voltage 22V, solution: 60 ml perchloric acid, 620 ml ethanol, 310 ml butyglycol. For TEM replicas, the specimens were thinned to about 40  $\mu$ m thickness and covered on both side with a thin carbon film. Then the matrix was dissolved in a solution of 10% bromium in ethanol. TEM investigation were carried out using a JEOL 200 CX and Philips CM200 combined with a Gatan Image Filter (GIF); the SEM investigations were carried out using LEO1530/Gemini microscope.

Specimens for SEM investigation were prepared to a polished surfaces and etched with 10% phosphoric acid at a voltage 3V. The measurement of particle sizes and the evaluation of size distributions were carried out by the image analysis system KS400 from Kontron. The images were taken on the electron microscopes in digital format or, if the contrast was too low, redrawn from a printed copy and scanned from the image analysis system.

In order to observe the phase transition and to verify the TTT diagrams from the literature, some experiments were carried out in a DTA (differential thermal analysis) facility. Specimens of 6 mm diameter and 10 mm length were heated up to the solvus temperature and cooled down

with different constant cooling rates. The temperature differences were measured against a standard specimen of Pt.

#### Results and discussion

#### Inconel 706A

Microstructure after heat treatment. The variant Inconel 706 A after heat treatment exhibited two types of precipitation, the coherent  $\gamma$ ' phase of Ni<sub>3</sub>(Ti, Al) and the metastable semi-coherent  $\gamma$ ' phase of Ni<sub>3</sub>(Nb, Ti). In Figures 2 and 3 TEM images of Inconel 706 A alloy are shown. The spherical precipitates observed inside the grains were identified as  $\gamma$ ' phase and the disc shaped precipitates as  $\gamma$ ' phase. The  $\gamma$ ' and  $\gamma$ ' particles were homogeneously distributed inside grains with volume fractions of about 3% for  $\gamma$ ' and 4% for  $\gamma$ '. The mean length of  $\gamma$ ' particles was about 20 nm and the diameter of the spherical  $\gamma$ ' particles about 10 to 15 nm. Figure 3 shows the orientation of  $\gamma$ ' particles related to the matrix where the coherent planes of  $\gamma$ ' are parallel to the <100> or <010> planes of the matrix.

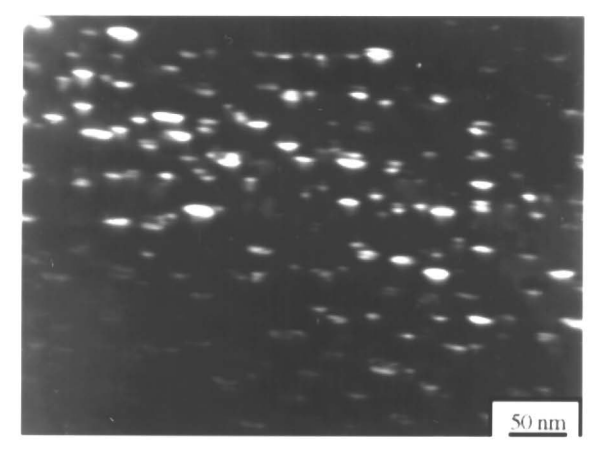


Figure 2: Homogeneously distributed  $\gamma$ ' and  $\gamma$ '' particles in Inconel 706 A (TEM dark field)

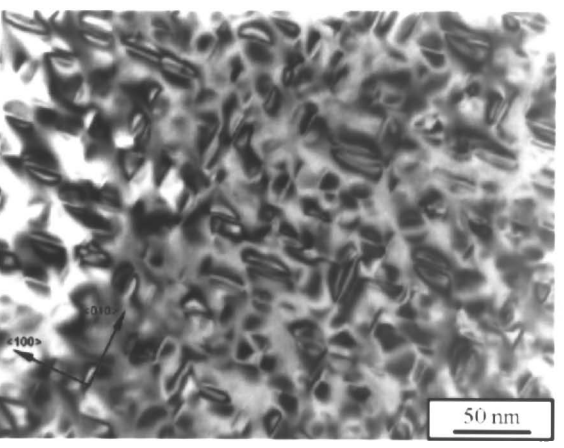


Figure 3: Coherence contrast of  $\gamma$ " particles demonstrates the orientation to the <100> and <010> directions in the matrix

Microstructure after ageing. To observe the structural changes in Inconel 706 A at elevated temperatures some ageing experiments were carried out at temperatures of 600, 650, 700 and

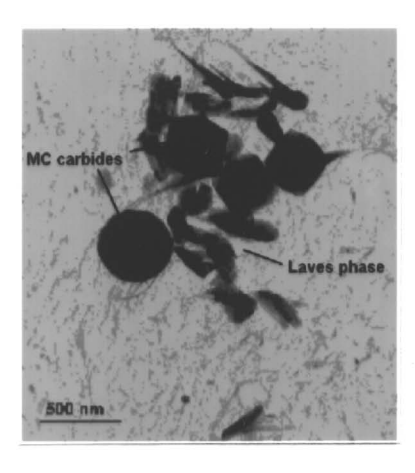


Figure 4: Laves plates in Inconel 706 A after 10000 h at 650°C (replica)

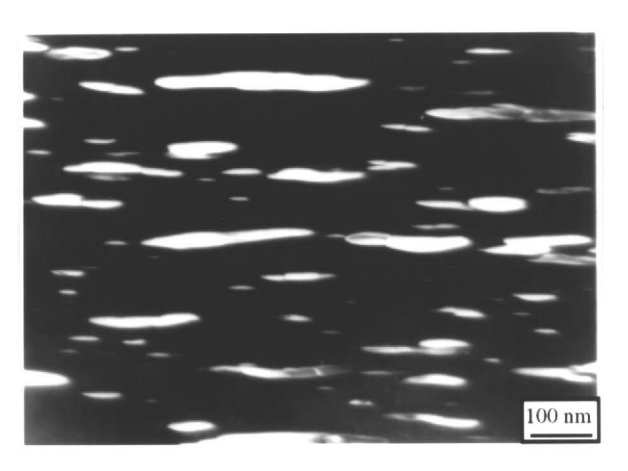


Figure 5: Microstructure of Inconel 706 A after ageing at 650°C and 30 000 h (TEM dark field)

750 °C with exposure times up to 30 000 h. At temperatures up to 620 °C and exposure times up to 10 00 h no significant changes of the  $\gamma$ ' and  $\gamma$ '' particle size was observed, but the Laves phase of the Fe<sub>2</sub>Nb type appeared at 600 °C after less than 3000 h. It was found as clusters of small platelets near to MC carbides. Figure 4 demonstrates this fact by a TEM replica image. where the larger particles are MC carbides and the small plates or needles are the Laves phase.

At temperatures of 650 °C and higher the  $\gamma$ " particles grew significantly. The changes in particle size and morphology in Inconel 706 A after ageing at 650°C and 30 000 h is presented in Figure 5. The main aspect of this image is the directional coarsening process of  $\gamma''$ . The  $\gamma''$ platelets grew in defined <001> direction of the matrix ( $\gamma$ ). This behavior can be explained by a minimization of coherency strain during the particle growth [6].

Table 3 and Figures 6 and 7 present the  $\gamma$ " particle size distribution and aspect ratio for Inconel 706 A in dependence on the exposure time and temperature.

Table 3: The changes in y'' size (length) and aspect ratio during long term ageing at 650 °C

	Time (h)	3000h	10000h	30000h
as received	Temperature (°C)	650	650	650
$18.1 \pm 9.8$	γ" particle length	$44.1 \pm 29.8$	$93.6 \pm 74$	$155.6 \pm 142$
$0.42 \pm 0.14$	particle aspect ratio	~0.4	~0.3	$0.24\pm0.12$

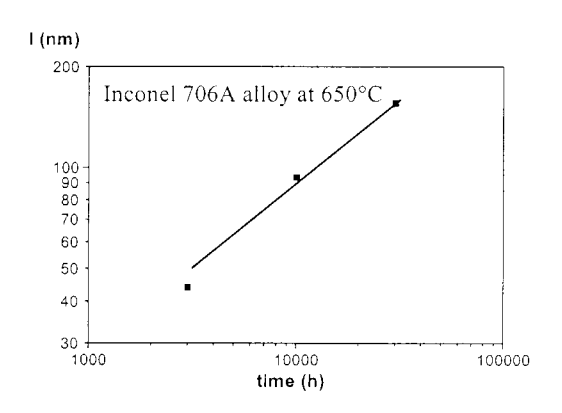
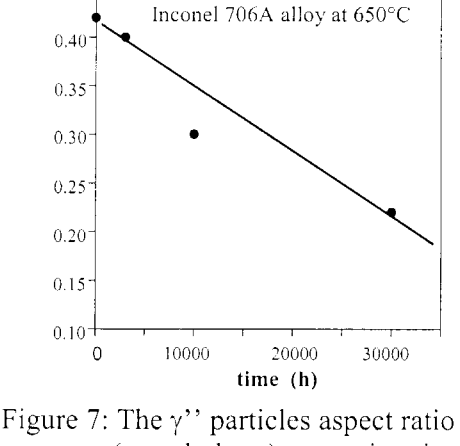


Figure 6: The growth of γ'' precipitates in Inconel 706 A alloy aged at 650°C.



aspect ratio

(morphology) vs. ageing time

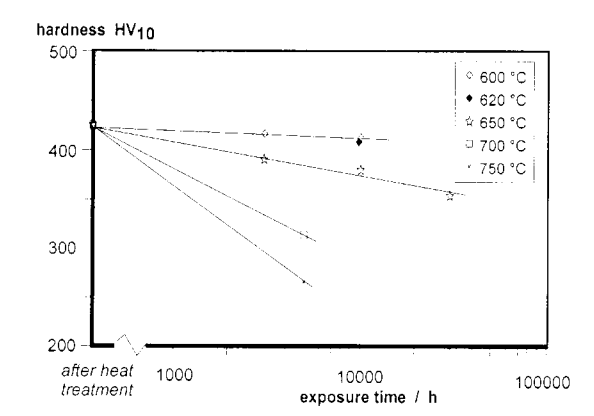


Figure 8: Hardness in dependence on ageing time and temperature

The results confirm the preferred growing directions for  $\gamma$ " phase during coarsening. The regression analysis shown in Figure 6 results to the equation  $1 = 0.547 t^{1/2}$ represents the particle length. This result is different to the growth of  $\gamma$ '-particles in a number of Ni-base alloys following the  $d \propto t^{1/3}$  rule of the LSW theory [7, 8] and is in agreement with the observation of a mainly planar growth of the y" particles. This result agrees with the Gibbs-Thompson theory [6] were the driving force for the planary growth is the minimization of the coherency strain.

At temperatures above 650 °C and after exposure times of about 3000 h the  $\eta$  phase appeared additionally on grain boundaries and twins. The volume fraction was very small and could not be measured. At 700 °C and more than 4000 h  $\eta$  phase appeared homogeneously distributed in the grain interior. Figure 8 demonstrates the loss of hardness in dependence on ageing temperature and time. The coarsening of  $\gamma$ ' and  $\gamma$ '' at 600 °C to 650 °C caused only a small loss of hardness. At temperatures higher than 650 °C the transformation to  $\eta$  phase occurred and led to a stronger decrease of hardness.

#### Inconel 706 B

microstructure after heat treatment. A typical microstructure of Inconel 706 B is represented by Figure 9. The  $\gamma$ ' and  $\gamma$ '' particles were homogeneously distributed in the  $\gamma$  matrix and exhibited a typical spherical ( $\gamma$ ') or prismatic ( $\gamma$ '') shape with sizes from 30 to 50 nm. The  $\eta$  phase precipitated at the grain boundaries in a cellular manner (Figure 9) or as a grain boundary film, dependent on the grain boundary orientation.

The platelets grow parallel to the (111) and had one partly coherent interface with the {111} plane The orientation relationship between  $\gamma$  and  $\eta$  phases is given by the relationship  $<0.11>_{\gamma}||<2.110>_{\eta}$ ,  $<1.11>_{\gamma}||<0.001>_{\eta}$  and was established using electron diffraction technique.



Figure 9: Microstructure of Inconel 706 B after heat treatment with cellular η phase at the grain boundary

Microstructure after ageing. In addition to the coarsening of  $\gamma$ ' and  $\gamma$ '' procedures as described in the section Inconel 706 A for an ageing temperature of 650 °C, the transformation of  $\gamma$ ' into the  $\eta$  phase becomes more important for higher ageing temperatures. In Figures 10 and 11 the microstructural features of Inconel 706 B alloy after ageing at temperatures of 700 and 750 °C for different ageing times are given.

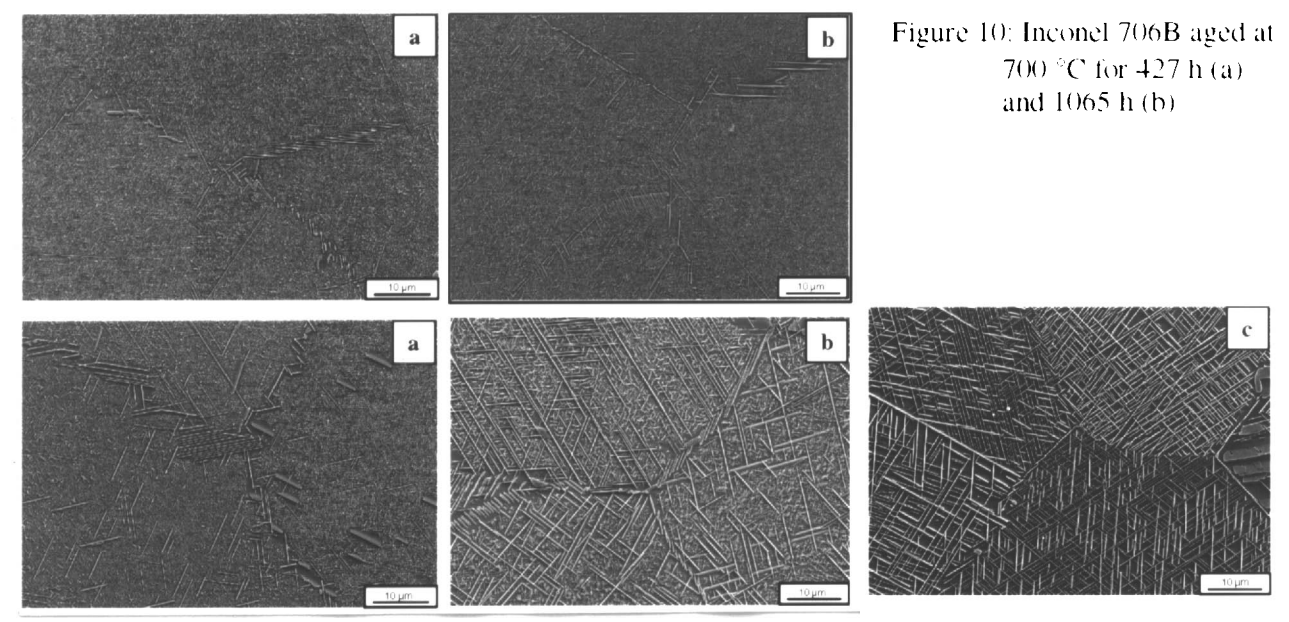


Figure 11: Inconel 706 B aged at 750 °C for 297 h (a), 955 h (b) and 2330h (c).

The influence of temperature on the transformation to the  $\eta$  phase is well documented by the comparison of Figures 10b and 11b (both specimens were aged with a similar duration). The amount of  $\eta$  phase after ageing at 750 °C was much higher than that after ageing at 700 °C. At 750 °C after 2330 h, the transformation to the  $\eta$  phase was nearly completed. More information was revealed from the TEM images (Figures. 12 and 13). The  $\gamma$ ' and  $\gamma$ '' particles were still

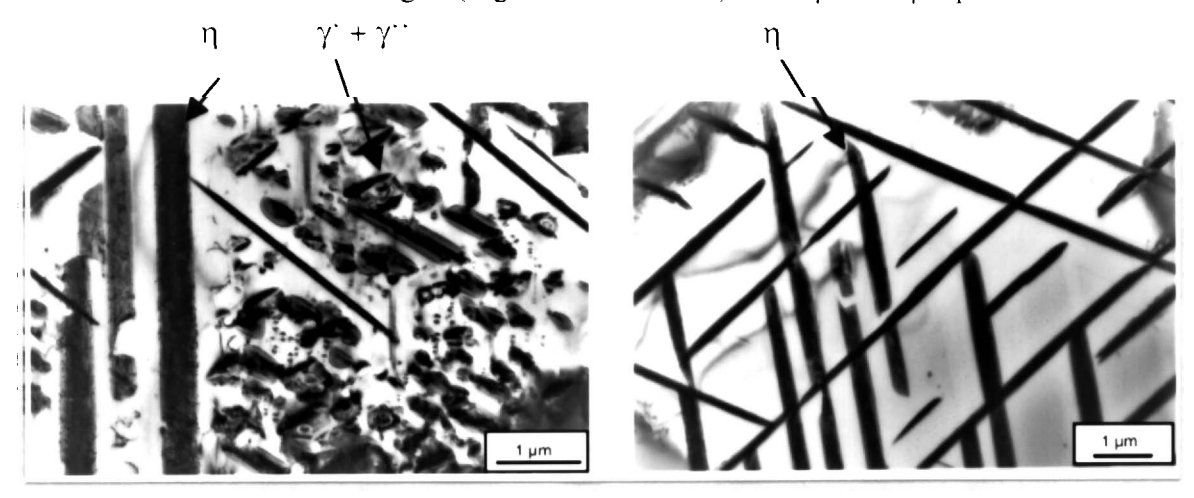


Figure 12: Inconel 706 B aged at 750 °C/2330 h

Figure 13: Inconel 706 B aged at 750 °C/5000 h

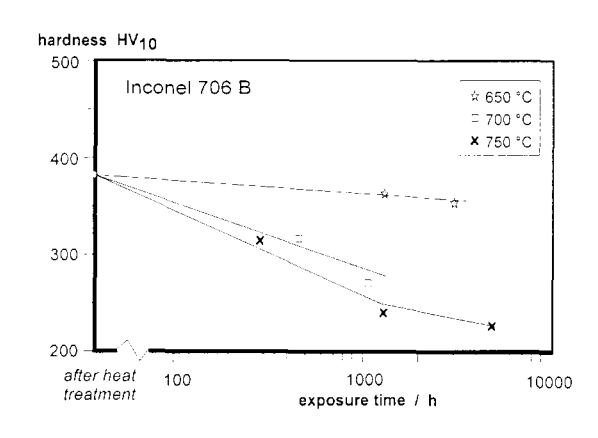


Figure 14: Hardness of Inconel 706 B in dependence on ageing time and temperature

visible between the η plates after 2330 h at 750 °C (Figure 12). In the case of extending the exposure time up to 5000 h, both of the strengthening phases  $\gamma$ ' and  $\gamma$ '' disappeared and the n phase dominated (Figure 13). It can be deduced that time needed to finish the transformation reaction in Inconel 706 B at 750 °C is between 3000 and 5000 h. Figure 14 shows the results of hardness measurements. The hardness Inconel 706 B after heat treatment is lower than that of Inconel 706 A and the loss of hardness in dependence on exposure time temperature indicates the same dependence on n phase transformation as with Inconel 706 A.

#### Inconel 706 C

Microstructure after heat treatment. The variant Inconel 706 C with increased Nb and C content contained after heat treatment an increased volume fraction of MC carbides than in Inconel 706 A or B and γ'' particles with a bimodal size distribution. The TEM dark field image of Inconel 706 C shown in Figure 15 demonstrates this fact. The primary γ'' reached a length of about 430 nm and the

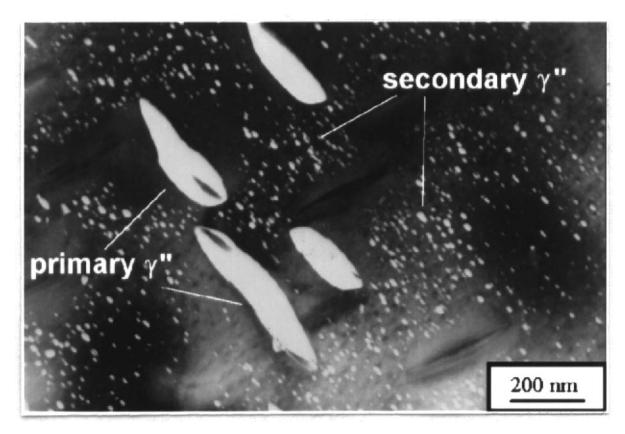


Figure 15: The microstructure of Inconel 706C after heat treatment type B

small secondary  $\gamma$ " precipitates showed a mean size of about 20nm. This precipitation behavior can be explained by an increase of the solvus temperature of  $\gamma$ " with increasing Nb content. It was expected that the  $\gamma$ " precipitation process occurred during the stabilization annealing and the primary  $\gamma$ " grow fast. During the subsequent annealing at 720 °C and 620 °C the secondary  $\gamma$ " were precipitated from the supersaturated solution. More detailed investigation of the coarsening kinetic in Inconel 706 C were presented elsewhere [13]. There were no significantly differences detected in respect to the  $\eta$  phase formation and the  $\gamma$ ",  $\gamma$ " coarsening behavior compared to Inconel 706 B.

## <u>Waspaloy</u>

Structure after heat treatment. The microstructure of Waspaloy after heat treatment consists of bimodal distribution of coherent  $\gamma$ ' particles Ni<sub>3</sub>(Ti,Al) with a volume fraction of about 0.25 and M<sub>23</sub>C<sub>6</sub> precipitates along the grain boundaries with a volume fraction below 0.002.

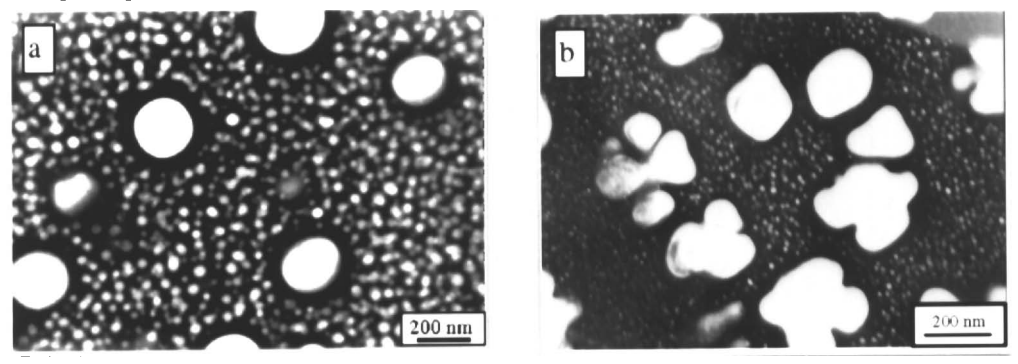


Figure 16: Microstructure of Waspaloy after heat treatment a) closed to surface and b) in the centre of a billet (TEM dark-field image).

Figure 16 shows TEM dark field images of  $\gamma$ ' precipitates in Waspaloy from specimens were took either from a surface near zone (a) or from the center (b) of a billet of 200 mm in diameter. The large  $\gamma$ ' precipitates, the primary  $\gamma$ ' differ obviously from the fine secondary  $\gamma$ '. The primary  $\gamma$ ' precipitates tended to form spheres in the specimen from the edge and more complex shapes in the billet center. The secondary  $\gamma$ ' particles center specimen were smaller compared to these in the surface specimen. It seems that the complex form of primary  $\gamma$ ' particles is a result of attraction of  $\gamma$ ' particles during the cooling down of the heat treatment.

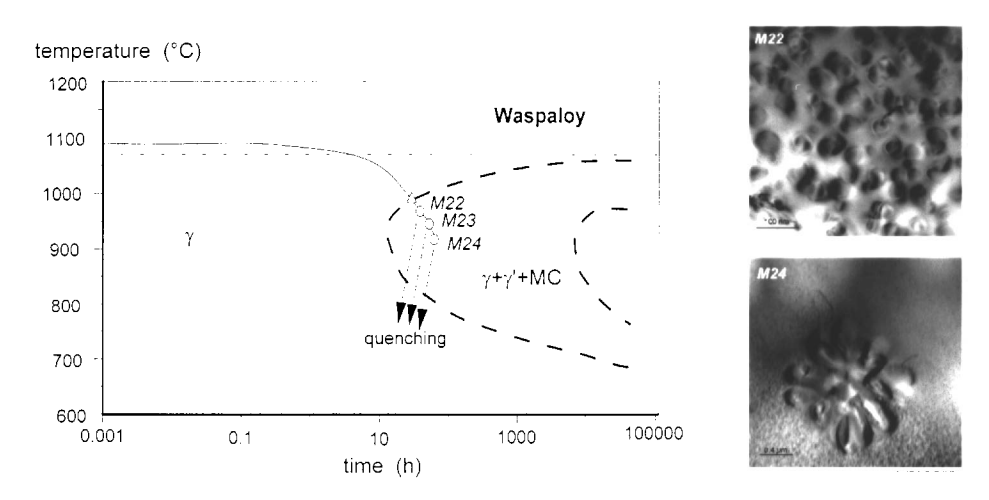


Figure 17: Scheme of cooling down in DTA experiments with Waspaloy. The TEM images show the resulting microstructure at the termination points M22 to M24.

In order to verify this assumption, the heat treatment steps were simulated in DTA experiments and the cooling rates after the solution annealing were varied. Figure 17 represents a simplified TTT diagram of Waspaloy; the cooling curve of three DTA experiments with an applied cooling rate of 0.1 K/min is drawn. The triangle marks the temperature for the  $\gamma$ ' precipitation and the circles mark the different terminations of the experiments by water quenching representing different cooling down durations. The structure images show the shape of the resulting  $\gamma$ ' particles.

The images of the experiment M22 terminated 1 h after the DTA signal (triangle) shows a homogeneous distribution of  $\gamma$ ' particles (about 30 – 50 nm). The image of M24 terminated 7.5 h after the DTA signal shows an attraction of  $\gamma$ ' particles to a local center. The driving force for this attraction might be the removal of the elastically strained matrix lying between two coherent particles if the lattice parameter were different in the precipitates and matrix i.e. the process will depend on the  $\gamma$ ' misfit [12].

Microstructure after ageing. In order to observe the ageing behavior of Waspaloy a set of creep specimens tested at 650, 700 and 750 °C were investigated. After 6700 h at 650 °C no significant change in  $\gamma$ ' particle amount and shape has been observed. After exposure at 700 °C a reduction of secondary  $\gamma$ ' and a coarsening of primary  $\gamma$ ' particles was detected. The volume fraction of secondary  $\gamma$ ' decreased from 4.8 % as received to about 0.1 % after 2500 h and the volume fraction of primary  $\gamma$ ' increases in the opposite way. After 5000 h at 750 °C the small secondary  $\gamma$ ' particles disappeared completely and the dimensions and volume fraction of large primary  $\gamma$ ' particles increased from 13.8% in as-received conditions to about 22-24%. That means that after heat treatment, the system is not in equilibrium state, not all of possible  $\gamma$ ' has been precipitated.

# IN 617 alloy

Microstructure after heat treatment. Inconel 617 is a solid solution hardened Ni-base alloy which is additionally strengthened by M(C,N)carbonitrides homogeneously distributed M<sub>23</sub>C<sub>6</sub> carbides with a size of about 60 - 100 nm (Figure 18). The distribution of carbides is dependent on the cooling rate after solution annealing and tend slightly to form clusters at lower cooling rates leading to differences in the hardness values within the grains. The influence of carbides mentioned above on the properties of Inconel 617 depends on their morphology. After heat treatment M<sub>23</sub>C<sub>6</sub> carbides are usually globular and strengthen the matrix and the grain boundaries. The volume fraction of M<sub>23</sub>C<sub>6</sub> carbides was estimated to be 0.006 - 0.007 [14]. The

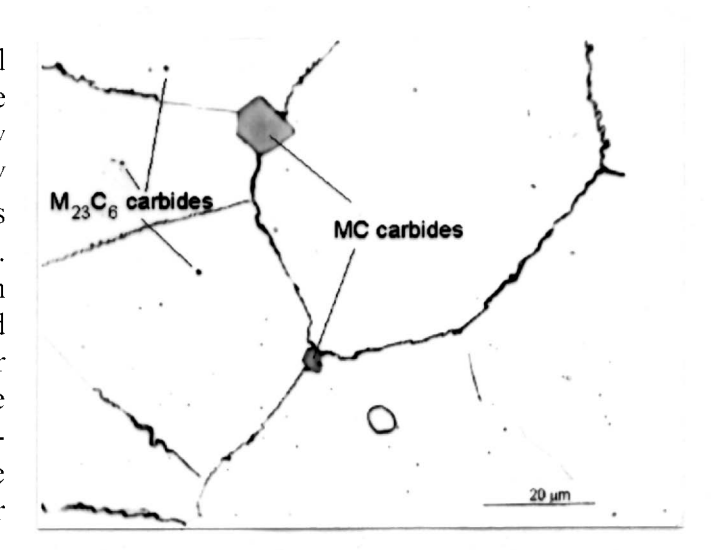


Figure 18: Micrograph of Inconel 617 showing M(C,N) carbonitrides and small M23C6 carbides

volume fraction of homogeneous distributed carbonitrides of the Ti(C,N) type was about 0.004 %. Because of the high Mo content the formation of  $M_6C$  carbides ( $Mo_6C$  type) is possible and has been detected (volume fraction about 0.001) in TEM analysis.

Microstructure after ageing. During the ageing at temperatures of 700 - 750 °C the  $M_{23}C_6$  carbides tended to grow along the grain to form of carbide film at the grain boundaries. Additionally lamellae structures of  $M_{23}C_6$  needles has been found (Figure 19). These kinds of  $M_{23}C_6$  structures has been observed even after an exposure of 100h (but in a smaller amount and size). The needle like carbides were clustered to islands and were oriented from the grain boundaries inside the grain interior and parallel to boundary.

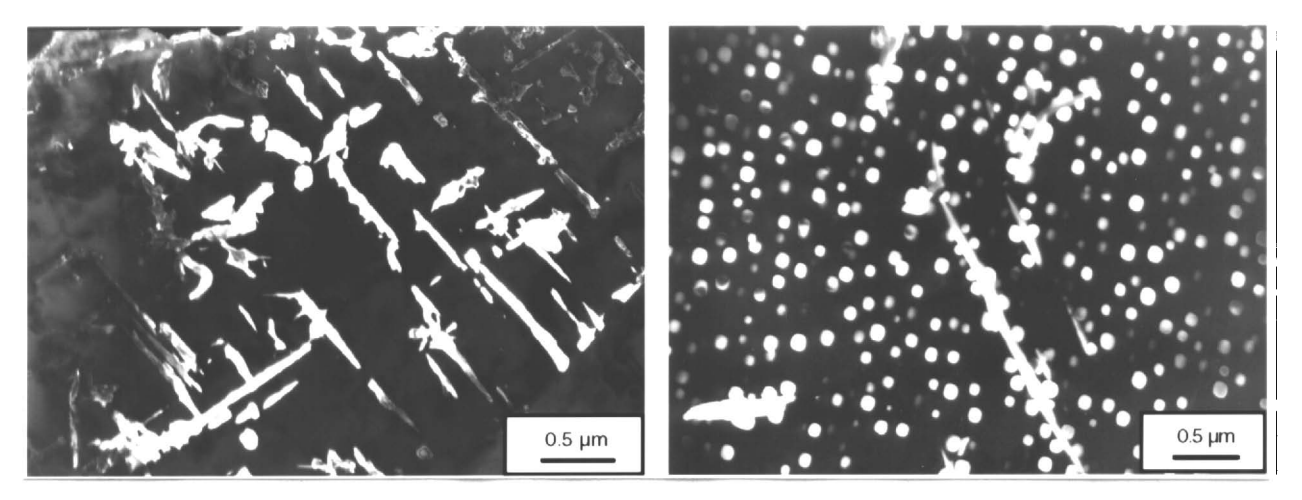


Figure 19: M<sub>23</sub>C<sub>6</sub> needles formed in Inconel 617 after 5000 h at 750 °C (TEM dark field)

Figure 20: Microstructure of Inconel 617 after 5000 h at 750 °C containing γ' particles and M23C6 needles (TEM dark field)

Two appearances of carbide precipitates at grain boundaries exist: the globular particles and the formation of films along the grain boundaries. It can be deduced that during long term service continuous carbide films will be formed.

An unexpected effect of the ageing of Inconel 617 at 700 to 750 °C was the precipitation and growth of very homogeneously distributed  $\gamma$ ' particles. The precipitation of  $\gamma$ ' particles of a mean size of about 20 nm was still observed after 83 h at 700 °C. After ageing at 750 °C and 5000 h  $\gamma$ ' particles with a size of about 80 – 90 nm and a volume part of about 4 % were detected (Figure 20).

#### **Conclusions**

Three Ni-base wrought alloys, Inconel 706, Waspaloy and Inconel 617, representative for alloys with different hardening mechanisms were investigated in respect to their microstructure and microstructural stability at temperatures from 650 °C to 750 °C. Inconel 706 is hardened by  $\gamma$ ',  $\gamma$ '' and  $\eta$  phases The presence of  $\eta$  phase along the grain boundaries can be controlled by the heat treatment. The microstructure is not stable at temperatures above 650 °C and the microstructural changes are characterized by particle coarsening after medium service life and long term phase transformation into the platelets forming  $\eta$  phase. An increase of the Nb content leads to a bimodal size distribution of  $\gamma$ '' particles and do not change the amount of  $\eta$  phase after heat treatment significantly.

The alloy Waspaloy exhibits a bimodal size distribution of primary and secondary  $\gamma$ ' particles strongly dependent on the cooling rate after solution annealing during the heat treatment. During service life at temperatures above 700 °C  $\gamma$ ' particles coarsen to a homogeneous microstructure containing with  $\gamma$ ' particles of about 250 nm diameter.

Inconel 617 is a solution hardened Ni-base alloy exhibiting small  $M_{23}C_6$  carbides after heat treatment. During service life above 700 °C the carbides tend to form carbide films at the grain boundaries and small needle like precipitates inside the grains. Because of the Al and Ti content of this alloy  $\gamma$ ' will be precipitated in a homogeneous distribution and a volume fraction of maximum 0.04.

### References

- [1] F. Tarcet, H.K.D.H. Bhadeshia and D.J.C. Mac Kay, "Design of new creep-resistant nickel-base superalloys for power plant applications", <u>Key Engineering Materials</u> 171-174 (2000), 529-536.
- [2] K.A. Heck, "The Time-Temperature-Transformation Behaviour of Alloy 706", Paper presented on the Conference Superalloys 718, 625, 706 and Various Derivatives, 1994, 393-404.
- [3] T. Takahashi et al., "Effects of Grain Boundary Precipitation on Creep Rupture Properties of Alloys 706 and 718 Turbine Disk Forging", Proc. Conf. Superalloys 718, 625, 706 and Various Derivatives, 1994, 557-565.
- [4] G.W. Kuhlman, "Microstructure-Mechanical Properties Relationships in Inconel 706 Superalloy" Proc. Conf. Superalloys 718, 625, 706 and Various Derivatives, 1994, 441-450.
- [5] T.Shibata, et al. "Effect of Stabilizing Treatment on Precipitation Behaviour of Alloy 706", Proc. Conf. Superalloys 1996, pp. 153-636.
- [6] J. Rys and K. Wiencek, <u>Koagulacja faz w stopach</u>, Wydawnictwo Slask, Poland, 1979)
- [7] I.M. Lifshitz, V.V. Slyozow "The Kinetics of Precipitation From Supersaturated Solid Solution", Journal Phys. Chem. Solids, 19 (1/2) (1961), 35-50
- [8] C. Wagner, "Theorie der Alterung von Niederschlägen durch Umlösen (Ostwald-Reifung)", Zeitschrift für Elektrochemie, 65 (7/8) (1961), 581-591
- [9] R. Cozar, A. Pineau, "Morphology of γ' and γ'' Precipitates and Thermal Stability of Inconel 718 Type Alloys", <u>Metallurgical Transactions</u> 4 (1973), 47-
- [10] J. P. Collier, "The Effect of Varying Al, Ti, and Nb Content on the Phase Stability of Inconel 718", Metallurgical Transactions A 19A (1988), 1657-1666
- [11] C.T. Sims, "A perspective of Niobium in Superalloys", Proceedings of the International Symposium, Niobium'81, held in San Francisco, California, 8-11 November 1981, 1169-1211
- [12] R. D. Doherty, "Role of interfaces in kinetics of internal shape changes", Metal Science 16 (1982) 1-13
- [13] J. Wosik et al., "Stereological estimation of microstructural parameters of nickel-base superalloy Waspaloy using TEM methods", <u>Materials Characterization</u>, in press
- [14] F. Schubert, H. J. Penkalla, A. Weisbrodt "PHASCALC\*: An improved computer programme for the calculation of phase kinetics, microstructural parameters and microstructural instabilities in Nickel base Superalloys", Paper on the European Conference on Advanced Materials and Processes, Aachen, Germany, 1989,

# Acknowledgement

This work is part of the DFG - research programme "Herstellungs- und Lebensdauermodelle für den Einsatz von Nickel-basis Werkstoffen in Dampfturbinen oberhalb 700°C". The financial support of the Deutsche Forschungsgemeinschaft is gratefully acknowledged.